IOPscience iopscience.iop.org

Home Search Collections Journals About Contact us My IOPscience

Effects of the external magnetic field on the composition-fluctuation potentials in diluted magnetic semiconductors

This article has been downloaded from IOPscience. Please scroll down to see the full text article.

2006 J. Phys.: Condens. Matter 18 6621

(http://iopscience.iop.org/0953-8984/18/29/005)

View the table of contents for this issue, or go to the journal homepage for more

Download details:
IP Address: 129.252.86.83
The article was downloaded on 28/05/2010 at 12:22

Please note that terms and conditions apply.

INSTITUTE OF PHYSICS PUBLISHING JOURNAL OF PHYSICS: CONDENSED MATTER

J. Phys.: Condens. Matter **18** (2006) 6621–6634 doi:10.1088/0953-8984/18/29/005

Effects of the external magnetic field on the composition-fluctuation potentials in diluted magnetic semiconductors

Masakatsu Umehara

3-11-30 Koyadai, Tsukuba, Ibaraki 305-0074, Japan

Received 1 February 2006, in final form 16 May 2006
Published 30 June 2006
Online at stacks.iop.org/JPhysCM/18/6621

Abstract

We investigated the effects of the external magnetic field on the compositional-fluctuation potentials (APFs) in diluted magnetic semiconductors (DMSs). The APFs in DMSs are divided into two parts: one is the nonmagnetic part usually considered in mixed nonmagnetic semiconductors and the other is the magnetic part caused by the compositional fluctuations of the substituted magnetic ions and the sp–d exchange interaction under the external magnetic field. The APFs in DMSs, thus, depend on the external magnetic field and the temperature as well as the concentration of the magnetic ions; for example in $Cd_{1-x}Mn_xTe$, the APFs increase with the magnetic field up to about 40 kOe for an Mn concentration of $x = 0.2$ and 0.3, while the APFs decrease drastically with the magnetic field for x less than 0.05 at low temperatures. After a general discussion of the APFs in DMSs, we calculated the exciton magnetic polarons weakly bound to APFs under the external magnetic field. The calculated results were compared with the experiment on the L_2 photoluminescence in $Cd_{1-x}Mn_xTe$, with the purpose of revealing the peculiar properties caused by the magnetic part of the APFs.

1. Introduction

There have been continuing interests in the optical, magnetic and transport properties of diluted magnetic semiconductors (DMSs), due to their possible application in devices as well as their importance in basic research [1]. In DMSs, some of the cations are substituted randomly by transition metal ions with localized magnetic moments such as the ternary alloy $Cd_{1-x}Mn_xTe$; the electrons, the holes and the excitons in DMSs strongly interact with the magnetic moment through the so-called sp–d exchange interaction, producing substantial variation in their properties. At the same time, the randomly substituted transition metal ions inevitably produce the potential fluctuations due to the local compositional fluctuation of the transition metal ions (referred hereafter as alloy potential fluctuations, abbreviated to APFs) [2, 3]. As a result,

 © 2006 IOP Publishing Ltd Printed in the UK

an electron, a hole and an exciton with low kinetic energy may be bound in the potential well caused by the APFs. In a previous paper [4], the present author theoretically studied the exciton magnetic polarons (EXMPs) in DMSs weakly bound to APFs for the case without an external magnetic field. The calculated Stokes shift was in good agreement with the Stokes shift measured for the L_2 luminescence after the interband excitation in $Cd_{1-x}Mn_xTe$ [5]. Then, the exciton with the low kinetic energy is affected by the APFs. Since transition metal ions such as Mn ions are magnetic, are the APFs in DMSs influenced by the external magnetic field? In this paper, thus, we investigate how the APFs in DMSs are affected by the external magnetic field. The paper is organized as follows. In section 2, the localization energies caused by the APFs obtained from the experiments with and without a magnetic field are summarized for $Cd_{1-x}Mn_xTe$. In section 3, the exciton–APF interaction in DMSs is studied under an external magnetic field: the interaction is divided into nonmagnetic and magnetic parts. The latter is caused by compositional fluctuations of the substituted magnetic ions and the sp–d exchange interaction. In section 4, the EXMPs weakly bound to APFs are calculated under the external magnetic field for $Cd_{1-x}Mn_xTe$. The result is compared with the Stokes shift of the L_2 photoluminescence observed after the interband excitation with the purpose of revealing the effect of the magnetic part of the APFs in the experiment. The localization energies summarized in section 2 are also compared with the calculation. A summary is given in section 5. The effects studied here may also influence the EXMPs after selective excitation [6, 7], and these may be rather strongly bound to the APFs. Such a case, however, is not the concern of this paper.

2. Localization energies due to APFs obtained by experiments

In determining the localization energy of the exciton caused by the APFs, the following two methods using the transient luminescence technique have been reported. The first method estimates the localization energy from the energy shift of the L_2 luminescence in the high temperature regions where the energy shift is insensitive to temperature [8, 9]. For example, in $Cd_{0.88}Mn_{0.12}Te$ [8], the energy shift below 20 K increases drastically with decreasing temperature by the formation of EXMPs, while the energy shift above 20 K is insensitive to temperature. The authors [8, 9] considered that the temperature-insensitive shift above 20 K is due to the localization of APFs without the magnetic polaron effect. The second method estimates the localization energy from the energy shift of the luminescence at high magnetic fields [10, 11]. For example, in $Cd_{0.9}Mn_{0.1}Te$ [10], the localized magnetic moments of Mn ions are almost saturated by the magnetic field of 70 kOe. In this case, the localization energy does not contain the magnetic polaron effect; the energy shift estimated at 70 kOe is, thus, considered as the localization energy of the APFs. Then, the question arises of whether the two methods above give the same APF localization energy. To examine this in short, we summarize the localization energy caused by the APFs in $Cd_{1-x}Mn_xTe$ reported so far in figure 1 as a function of Mn concentration. In figure 1, the closed and the open circles show the localization energy estimated from the L_2 photoluminescence experiment: the closed circles were obtained using the first method during 300 ps [8, 9], while the open circles are from the second method [10, 11]—the lower open circles are during 300 ps, while the upper are during 1.5 ns. (The localization energy during 1.5 ns is considered to include the effect of the exciton migration [12].) The APFs also bring about the smearing of the absorption edge: the closed squares with the dotted line show the half-width of the reflection spectra of $Cd_{1-x}Mn_xTe$ at 0 kOe [13], which is taken as half of the distance between the maximum and the minimum in the dispersion structure. In addition, the solid line shows a measure of the band edge smearing [3]

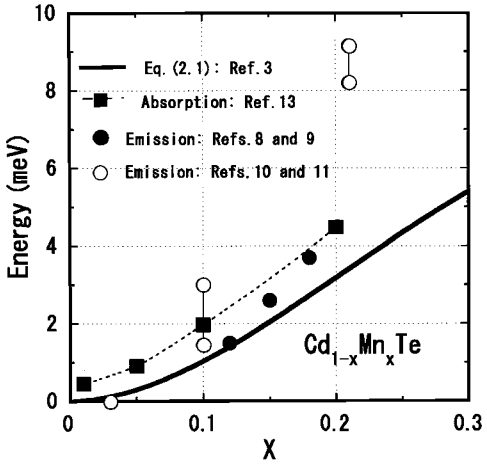

Figure 1. The localization energy caused by APFs is shown as a function of Mn concentration x together with the energy of the band edge smearing. The localization energy obtained at the high temperature region is shown by the closed circles, while that obtained at the high magnetic field is shown by the open circles. On the other hand, the energy of the band edge smearing is shown by the solid line and the closed squares with the dotted line.

given by

$$E_0 = \frac{1}{(176 \times 16)E_{\mathrm{H}}^3}\xi^4 x^2(1-x)^2\left(\frac{m_{\mathrm{e}}+m_{\mathrm{h}}}{m}\right)^3\left(\frac{\mathrm{d}(x)}{a_{\mathrm{B}}}\right)^6. \tag{2.1}$$

The localization energy caused by the APFs is measured downwards in the bandgap from the edge of the extended states; the state density of the localized states at E_0 becomes $1/e$ compared with the density of the state at the edge of the extended states [3]. In equation (2.1), $\xi = \frac{\mathrm{d}E_{\mathrm{g}}}{\mathrm{d}x}$ is the coefficient of the exciton–APF interaction, m_{e} (m_{h}) is the effective mass of the electron (hole), E_{g} is the bandgap between the conduction and the valence bands, E_{H} is the Rydberg constant of 13.6 eV, x is the concentration of the magnetic ions and the other notations is the same as in [4]. From figure 1, we see that:

(i) All the plots obtained from the experiment are roughly approximated by the theoretical line [3] within 1 meV except the open circle for $x = 0.21$.

(ii) The localization energy indicated by the closed circle for $x = 0.12$, obtained by the first method, is roughly the same as the localization energy indicated by the lower open circle for $x = 0.1$ obtained by the second method at 4.5 K with 70 kOe.

(iii) However, the localization energy indicated by the lower open circle for $x = 0.21$, obtained by the second method at 4.5 K with 65 kOe, is remarkably different from the localization energy indicated by the closed circle for $x = 0.18$ obtained by the first method.

(iv) The localization energy by the open circle for $x = 0.03$ [11] obtained by the second method at 4.2 K with 70 kOe is negligibly small compared with the energy of the band edge smearing obtained from the reflection spectra [13].

What kind of relation is there between the localization energies obtained by the first and the second methods? We will discuss the relation in sections 3 and 4.

3. Exciton–APF interaction in DMSs

In this section, the exciton–APF interaction in DMSs is studied under an external magnetic field. The APFs for an exciton may be written as [14]

$$V(\vec{r}) = \bar{V} + v(\vec{r}), \tag{3.1}$$

where $\bar{V}$ is the average potential over the crystal and

$$v(\vec{r}) = \left[\frac{\mathrm{d}V}{\mathrm{d}x}\right]_{\Delta x(r)=0} \Delta x(\vec{r}). \tag{3.2}$$

Here $\Delta x(\vec{r}) \equiv x(\vec{r}) - x$ is the local compositional fluctuations of the substituted magnetic ions at $\vec{r}$, and x is the average composition (hereafter, the magnetic ions are assumed to be Mn ions). $\bar{V}$ is approximated by the excitation energy from the top of the valence bands to the bottom of the conduction bands, i.e. the energy of the bandgap, E_{g}. Then the exciton–APF interaction is rewritten as

$$H_{\mathrm{EX-APFs}} = \xi \Delta x(\vec{r}), \tag{3.3}$$

with $\xi = [\frac{\mathrm{d}E_{\mathrm{g}}}{\mathrm{d}x}]$. Let us remember that the bandgap in DMSs also depends on the external magnetic field through the sp–d exchange interaction. By taking account of this, the bandgap under a magnetic field of H may be given by

$$E_{\mathrm{g}} = E_{g0} - \frac{1}{2} N_0 \left[\alpha \tanh\left(\frac{\Delta_{\mathrm{e}}^0}{kT}\right) + \beta \tanh\left(\frac{\Delta_{\mathrm{h}}^0}{kT}\right)\right] x_{\mathrm{eff}} SM(H), \tag{3.4}$$

where E_{g0} is the bandgap without the magnetic field, $N_0\alpha$ ($N_0\beta$) is the coefficient of the s(p)–d exchange interaction between electron (hole) and Mn spins, x_{eff} is an effective Mn concentration [15], S is the magnitude of the Mn spin, and $M(H)$ is the magnetization of Mn under a uniform external magnetic field calculated by the Brillouin function B_S as

$$M(H) = B_S(\lambda). \tag{3.5}$$

Here λ is the molecular field given by

$$kT\lambda = g_{\mathrm{Mn}}\mu_{\mathrm{B}} HS - \frac{3S}{S+1} k\Theta_{\mathrm{AF}} M(H), \tag{3.6}$$

with the effective antiferromagnetic temperature Θ_{AF} [16]. Two results for x_{eff} are shown in figure 2(a) as a function of x: case (1) is a result of an analytical calculation by Shapira *et al* [17], which agrees with the experiment up to $x = 0.1$, while case (2) is the result of a simulation by Fata *et al* [18], which agrees with the experiment up to $x = 0.3$. Here we use case (2) for the calculation. Θ_{AF} also depends on x as $\Theta_{\mathrm{AF}}(x) = (37.45 \pm 1.06)x$ (K) between $x = 0.005$ and 0.2 for $Cd_{1-x}Mn_xTe$ (see appendix in [19]). Furthermore, Δ_{e}^0 (Δ_{h}^0) is the spin-splitting [20] of the electron (hole), defined by $\Delta_{\mathrm{e}}^0 = \frac{N_0\alpha}{2} x_{\mathrm{eff}} SM(H) + \frac{1}{2} g_{\mathrm{e}}\mu_{\mathrm{B}} H$ or $\Delta_{\mathrm{h}}^0 = \frac{N_0\beta}{2} x_{\mathrm{eff}} SM(H) + \frac{1}{2} g_{\mathrm{h}}\mu_{\mathrm{B}} H$, k is the Boltzmann constant, T is the temperature, $g_{\mathrm{e}}(g_{\mathrm{h}})$ is the g-factor of the electron (hole), μ_{B} is the Bohr magneton, and $\tanh(\frac{\Delta_{\mathrm{e}}^0}{kT})$ and $\tanh(\frac{\Delta_{\mathrm{h}}^0}{kT})$ give, respectively, the degree of spin polarization of the electron and hole. The magnetization $M(H)$ calculated at 2 K is shown in figure 2(b) as a function of x for several H; the x dependence of $M(H)$ is due to the x dependence of Θ_{AF}. We assume, hereafter, that $E_{g0} = 1.595 + 1.59x$ (eV) for $Cd_{1-x}Mn_xTe$ [21]. In figure 3 the x dependence of the bandgap, $E_{\mathrm{g}}(x) - E_{\mathrm{g}}(x = 0)$, is shown, which is calculated at 2 K with $N_0\alpha = 220$ meV and $N_0\beta = -880$ meV for $Cd_{1-x}Mn_xTe$ [16].

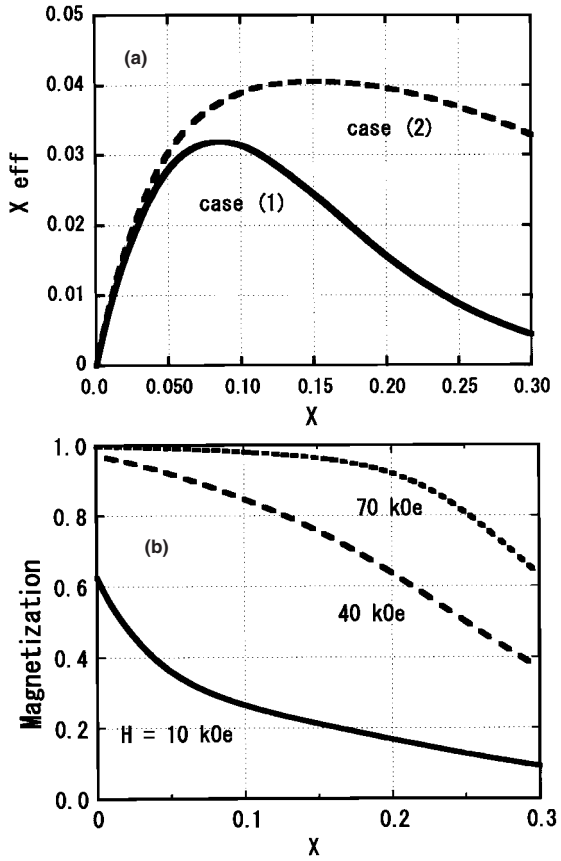

Figure 2. The effective concentration of Mn ions x_{eff} and the magnetization of Mn spins for various magnetic fields are shown in (a) and (b), respectively, as a function of Mn concentration x. Consult the text for the definition of cases (1) and (2) in (a).

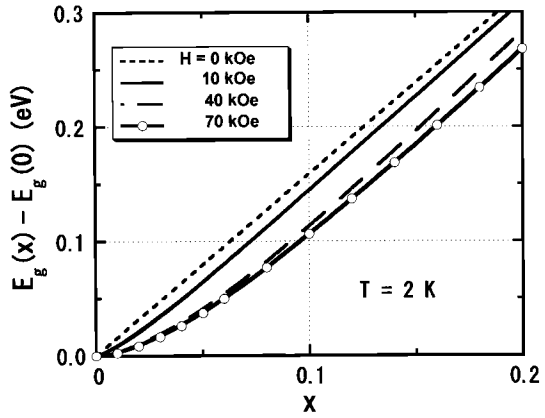

Figure 3. The x dependence of the bandgap, $E_{\mathrm{g}}(x) - E_{\mathrm{g}}(0)$, calculated at 2 K is shown for various magnetic fields.

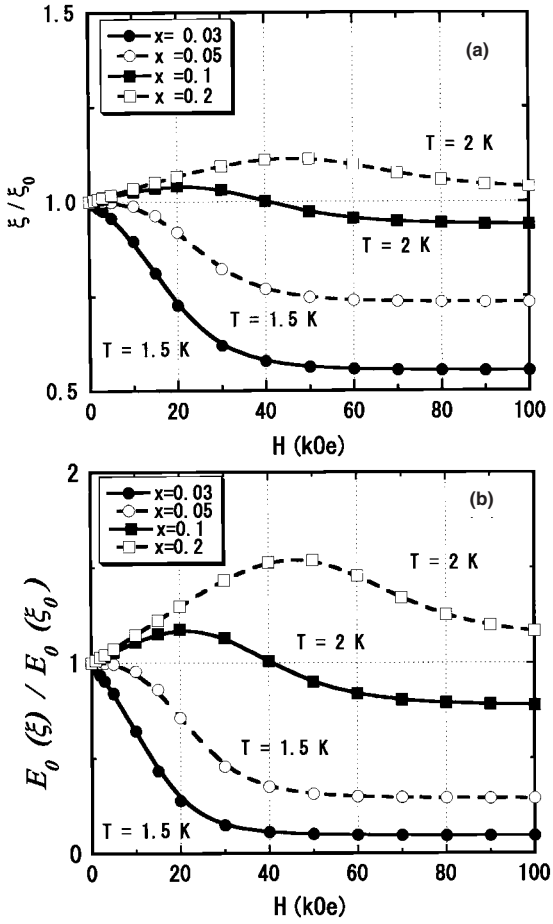

Figure 4. The coefficient of the exciton–APF interaction normalized by that of the nonmagnetic part, ξ/ξ_0, is shown in (a) at 1.5 and 2K, while $E_0(\xi)/E_0(\xi_0)$ is shown in (b) as a function of H for various x.

Now, the coefficient ξ of the exciton–APF interaction under the external magnetic field is given by

$$\xi = \frac{\mathrm{d}E_\mathrm{g}}{\mathrm{d}x} = \frac{\mathrm{d}E_{g0}}{\mathrm{d}x} - \frac{1}{2}N_0 S\frac{\mathrm{d}}{\mathrm{d}x}\left\{\left[\alpha\tanh\frac{\Delta_\mathrm{e}^0}{kT} + \beta\tanh\frac{\Delta_\mathrm{h}^0}{kT}\right]x_\mathrm{eff}M(H)\right\}. \tag{3.7}$$

Thus, ξ is divided into a nonmagnetic part, $\xi_0 = \frac{\mathrm{d}E_{g0}}{\mathrm{d}x}$, and a magnetic part due to the sp–d exchange interaction given by the second term of the right-hand side in equation (3.7). The former has been considered in mixed nonmagnetic semiconductors [3, 14]; however, the latter is characteristic of DMSs. Note that both x_eff and $M(H)$ depend on x as shown in figure 2. In figure 4(a), the calculated magnetic field dependence of ξ normalized by ξ_0 is shown for various x for $\mathrm{Cd}_{1-x}\mathrm{Mn}_x\mathrm{Te}$ with $\xi_0 = 1.59\ \mathrm{eV} > 0$. Typical cases are discussed below:

(i) At low temperatures such as $|\tanh(\frac{\Delta_\mathrm{e}^0}{kT})|, |\tanh(\frac{\Delta_\mathrm{h}^0}{kT})| \cong 1$, which are easily realized in DMSs, ξ is approximated as

$$\xi = \xi_0 - \frac{1}{2}N_0(\alpha-\beta)S\left[M(H)\frac{\mathrm{d}x_\mathrm{eff}}{\mathrm{d}x} + x_\mathrm{eff}\frac{\mathrm{d}M(H)}{\mathrm{d}x}\right]. \tag{3.8}$$

Since $\frac{dx_{eff}}{dx}$ is positive for $x \leqslant 0.15$ but negative for $x \geqslant 0.15$ for case (2) in figure 2(a), the first term in the bracket of equation (3.8) leads to $\xi < \xi_0$ for $x \leqslant 0.15$, and $\xi > \xi_0$ for $x \geqslant 0.15$. (The sign of $\frac{d}{dx}x_{eff}$ in case (1), however, changes at $x \approx 0.08$.) On the other hand, the second term in the bracket is always negative and leads to $\xi > \xi_0$ for all x. The behaviour of ξ in figure 4(a) is, thus, explained as follows. For $x = 0.1$, the first term in the bracket in equation (3.8) is positive, while the second term is negative; the effects of the magnetic part of the APFs are partially cancelled and are thus relatively small for $x = 0.1$. For $x = 0.2$, since the first term is negative as well as the second term, the APFs increase as a whole due to the effects of the magnetic part of the APFs. Under closer observation for $x = 0.1$ and 0.2, at $H < 70$ kOe both the first and the second terms in the bracket contribute to ξ, while at $H > 70$ kOe the first term makes the main contribution. On the other hand, the behaviour for $x = 0.03$ and 0.05 is mainly due to the first term in the bracket with the positive sign, since the second term becomes less important due to fairly small x_{eff} in this region; ξ always becomes smaller than ξ_0 due to the magnetic part of the APFs.

(ii) In the region of quite low Mn concentration, where $x_{eff} \sim x$, $\xi = \xi_0 - \frac{1}{2}N_0(\alpha - \beta)S$ at such low temperatures or strong magnetic fields that $M(H)$ is almost saturated. Then ξ is reduced to about 30% of ξ_0 *at most* in $Cd_{1-x}Mn_xTe$, which may cause a remarkable change in the localized state assisted by the APFs.

(iii) For $Zn_{1-x}Mn_xS$ with a negative ξ_0, $|\xi|$ becomes larger than $|\xi_0|$ for $x \leqslant 0.15$, while $|\xi|$ becomes smaller than $|\xi_0|$ for $x \geqslant 0.15$ by the first term of the bracket in equation (3.8); this is opposite to the case for $Cd_{1-x}Mn_xTe$ discussed above.

(iv) At high temperatures such that $M(H) \approx 0$, ξ approaches the nonmagnetic part of the APFs, ξ_0. The measure of the band edge smearing E_0 in equation (2.1) is also changed by the external magnetic field, as shown in figure 4(b). The localization energy from the APFs obtained from the experiment by the first method mentioned in section 2 is derived from ξ_0, while the localization energy obtained by the second method is derived from ξ in a strong magnetic field. Both localization energies, thus, differ in principle. In this way, the APFs in DMSs are remarkably modified by the external magnetic field and the temperature. This is not the case in nonmagnetic mixed semiconductors such as $Cd_{1-x}Zn_xTe$.

4. Calculation for EXMPs weakly bound to APFs under an external magnetic field

4.1. Model and calculation

In section 3, we studied the exciton–APF interaction under an external magnetic field. When the magnetic field is so strong that all the magnetic moments of Mn-spins are completely polarized, the formation of EXMPs is impossible. In the other cases, however, the localization energy of the exciton is brought about by the EXMPs as well as the APFs. We thus extend the previous study of the EXMPs [4] to the case with an external magnetic field to investigate how the EXMPs are affected by the magnetic part of the APFs studied in section 3. We expect that the approximation in [4] is most accurate for $x \leqslant 0.1$ where the exciton binding energy is fairly larger than the localization energy by the APFs. However, we shall apply it over the range $0 \leqslant x \leqslant 0.3$ hereafter. According to [4], the following variation function for EXMPs is employed:

$$\begin{aligned}\phi(\vec{r}_e, \vec{r}_h) &= \phi_g(\vec{r}_g)\phi_r(\vec{r}_e - \vec{r}_h) \\ &= \left(\frac{v_g v_r}{\pi}\right)^{3/2} \exp\left\{-\tfrac{v_g^2}{2}\left[(1-\delta)\vec{r}_e + \delta\vec{r}_h\right]^2\right\} \exp\left\{-\frac{v_r^2}{2}(\vec{r}_e - \vec{r}_h)^2\right\} \qquad (4.1)\end{aligned}$$

in which $\phi_g(\vec{r}_g)$ and $\phi_r(\vec{r}_e - \vec{r}_h)$ are, respectively, the wavefunctions for the centre-of-mass motion and the relative motion of the exciton, and v_g, δ and v_r are, respectively, the variation parameters for each wave function. The free energy of the EXMPs under the magnetic field may be given as follows with a slight modification[1] of reference [4]:

$$\begin{aligned} F[\phi_g, \phi_r, M] = {} & \frac{3}{2}\frac{m}{m_e}E_H\left\{\left[(1-\delta)^2 + \frac{\delta^2}{\gamma_0}\right]v_g^2 + \left(1+\frac{1}{\gamma_0}\right)v_r^2\right\} \\ & - \frac{4}{\sqrt{\pi}}\frac{E_H}{\varepsilon}v_r - E_0(\xi_0)V_0\left(\frac{v_g^2}{(\bar{\sigma})^{-1}+v_g^2}\right) \\ & - kT\ln\left\{2\cosh\frac{\Delta_e}{kT}\right\} - kT\ln\left\{2\cosh\frac{\Delta_h}{kT}\right\} \\ & + \frac{3}{2}\left(\frac{S}{S+1}\right)\frac{1}{V_p}\int x_{\mathrm{eff}}(\vec{r})[k\Theta_{\mathrm{AF}}(x(\vec{r}))M(\vec{r})^2]\,\mathrm{d}\vec{r} \\ & - \frac{kT}{V_p}\int x_{\mathrm{eff}}(\vec{r})G(M(\vec{r}))\,\mathrm{d}\vec{r} - g_{\mathrm{Mn}}\mu_B H S\frac{1}{V_p}\int x_{\mathrm{eff}}(\vec{r})M(\vec{r})\,\mathrm{d}\vec{r}. \end{aligned} \tag{4.2}$$

Here, the first term is the loss of transfer energy by the localization of the exciton. The second is the attractive Coulomb interaction energy between the electron and the hole. The third term is the potential energy by the APFs, $V_{\mathrm{APFs}}(\vec{r})$, in which only the centre-of-mass motion is assumed to be affected by the APFs as in [4]. The fourth and fifth terms are the free energy due to the sp–d exchange interaction and the seventh and eighth terms are the magnetic energy and the entropy for Mn spins, respectively. The final term is the Zeeman energy for Mn spins. In equation (4.2), m is the free electron mass, $\gamma_0 = m_h/m_e$, V_p is the volume per cation and $G(M)$ is the magnetic entropy by the molecular-field approximation. $E_0(\xi_0)$ is the energy of the band edge smearing by the nonmagnetic part of the APFs, $V_0 = 18.7$ and $\bar{\sigma} = \sigma(\frac{m}{m_e+m_h})(\frac{E_H}{E_0})$ with $\sigma = 0.265$ [3, 22]. Moreover, $\Delta_e(\Delta_h)$ is the spin splitting of the electron (hole) including the Zeeman energy, defined by

$$\Delta_e = \frac{N_0\alpha}{2}S\int x_{\mathrm{eff}}(\vec{r})|\psi_e(\vec{r})|^2 M(\vec{r})\,\mathrm{d}\vec{r} + \frac{1}{2}g_e\mu_B H, \tag{4.3a}$$

$$\Delta_h = \frac{N_0\beta}{2}S\int x_{\mathrm{eff}}(\vec{r})|\psi_h(\vec{r})|^2 M(\vec{r})\,\mathrm{d}\vec{r} + \frac{1}{2}g_h\mu_B H, \tag{4.3b}$$

with $|\psi_e(\vec{r}_e)|^2 = \int|\phi(\vec{r}_e,\vec{r}_h)|^2\,\mathrm{d}\vec{r}_h$ and $|\psi_h(\vec{r}_h)|^2 = \int|\phi(\vec{r}_e,\vec{r}_h)|^2\,\mathrm{d}\vec{r}_e$, and $M(\vec{r})$ is the magnetization of the Mn spin calculated by equation (3.5) with

$$\begin{aligned} kT\lambda = {} & V_p\left\{\frac{N_0\alpha}{2}S|\psi_e(\vec{r})|^2\tanh\left(\frac{\Delta_e}{kT}\right) + \frac{N_0\beta}{2}S|\psi_h(\vec{r})|^2\tanh\left(\frac{\Delta_h}{kT}\right)\right\} \\ & + g_{\mathrm{Mn}}\mu_B H S - \frac{3S}{S+1}k\Theta_{\mathrm{AF}}(x(\vec{r}))M(\vec{r}). \end{aligned} \tag{4.4}$$

It must be noted that for the case of $\xi_0 > 0$, as in $Cd_{1-x}Mn_xTe$, the excitons are localized by APFs in the regions given by equation (4.5) where the local composition of Mn ions is less than the average one [22, 23]:

$$\Delta x(\vec{r}) = V_{\mathrm{APFs}}(\vec{r}')/\xi_0 = -|E|V_0\exp\left(-\frac{(\vec{r}')^2}{\sigma}\right)/\xi_0, \tag{4.5}$$

where $r' = r\sqrt{2(m_e+m_h)|E|}/\hbar$ with the approximation $|E| = E_0(\xi_0)$ as in [4]. The local compositional fluctuations also cause the local fluctuations of the effective Mn concentration

[1] In the present paper, we include the magnetic strain energy caused by the weak antiferromagnetic interaction between Mn spins.

$x_{\rm eff}(\vec{r})$ and the effective antiferromagnetic temperature $\Theta_{\rm AF}(x(\vec{r}))$, which are taken into account in equations (4.2)–(4.4). On the other hand, the free energy for the free exciton state, F_X, is defined as

$$F_X = -\frac{8}{3\pi\varepsilon^2}E_{\rm H}\frac{m_{\rm e}m_{\rm h}}{m_{\rm e}+m_{\rm h}} - kT\ln\left\{2\cosh\frac{\Delta_{\rm e}^0}{kT}\right\} - kT\ln\left\{2\cosh\frac{\Delta_{\rm h}^0}{kT}\right\} + \frac{3}{2}\left(\frac{S}{S+1}\right)x_{\rm eff}N_0k\Theta_{\rm AF}(x)M_X^2 - kTx_{\rm eff}N_0G(M_X) - g_{\rm Mn}\mu_{\rm B}HSx_{\rm eff}N_0M_X. \tag{4.6}$$

Here, N_0 is the number of cations per unit volume, and M_X is the magnetization of Mn spin in the free exciton state under an external magnetic field given by equations (3.5) and (3.6). By minimizing equation (4.2) with respect to $v_{\rm g}$, δ and v_r, we obtain the minimum free energy of the EXMPs under the magnetic field. In the optical experiment, the localization energy may be estimated from the difference in photon energy between the absorption and the emission, that is the Stokes shift. The photon energy to create the 1s free exciton may be given by

$$h\nu_a = E_{g0} - \frac{8}{3\pi}\frac{1}{\varepsilon^2}\frac{m_{\rm e}m_{\rm h}}{m_{\rm e}+m_{\rm h}}E_{\rm H} - \Delta_{\rm e}^0\tanh\left(\frac{\Delta_{\rm e}^0}{kT}\right) - \Delta_{\rm h}^0\tanh\left(\frac{\Delta_{\rm h}^0}{kT}\right). \tag{4.7}$$

On the other hand, the emission energy from the EXMPs is given by

$$h\nu_{\rm e} = E_{g0} + \frac{3}{2}\frac{m}{m_{\rm e}}E_{\rm H}\left\{\left[(1-\delta)^2+\frac{\delta^2}{\gamma_0}\right]v_{\rm g}^2 + \left(1+\frac{1}{\gamma_0}\right)v_r^2\right\} - \frac{4}{\sqrt{\pi}}\frac{E_{\rm H}}{\varepsilon}v_r - E_0(\xi_0)V_0\left(\frac{v_{\rm g}^2}{(\bar{\sigma})^{-1}+v_{\rm g}^2}\right) - \Delta_{\rm e}\tanh\left(\frac{\Delta_{\rm e}}{kT}\right) - \Delta_{\rm h}\tanh\left(\frac{\Delta_{\rm h}}{kT}\right). \tag{4.8}$$

In the present paper, the Stokes shift $h\nu_a - h\nu_{\rm e}$ is calculated for the following three cases. In case A, only the nonmagnetic part of the APFs is taken into account for the APF potential together with the homogeneous distribution of Mn ions for the magnetic system: $x(r) = x$ and $x_{\rm eff}(r) = x_{\rm eff}$ in equations (4.2)–(4.4). The magnetic part of the APFs, is thus not considered in case A. In case B, although only the nonmagnetic part of the APFs is considered for the APF potential as in case A, the local compositional fluctuations of Mn ions, $\Delta x(r)$, are taken into account by equation (4.5) for the magnetic system. The effects of the magnetic part of the APFs are, thus, implicitly taken into account. On the other hand, in case C, both the nonmagnetic and the magnetic parts of the APFs are explicitly considered for both the APF potential and the local compositional fluctuations of Mn ions: ξ_0 in equations (4.2) and (4.5) is replaced with ξ in equation (3.7). Instead, for case C, the following portion of the sp–d exchange energy associated with the APFs potential,

$$-\frac{1}{2}N_0\alpha S\frac{\rm d}{{\rm d}x}\left\{\tanh\frac{\Delta_{\rm e}^0}{kT}x_{\rm eff}M(H)\right\}\int\Delta x(\vec{r})|\psi_{\rm e}(\vec{r})|^2\,{\rm d}\vec{r} - \frac{1}{2}N_0\beta S\frac{\rm d}{{\rm d}x}\left\{\tanh\frac{\Delta_{\rm h}^0}{kT}x_{\rm eff}M(H)\right\}\int\Delta x(\vec{r})|\psi_{\rm h}(\vec{r})|^2\,{\rm d}\vec{r} \tag{4.9}$$

is subtracted from the sp–d exchange energy in equations (4.2) and (4.8).

4.2. Calculated results and discussion

First, we show the Stokes shift calculated at 2 K for $x = 0.1$ in figure 5(a), for $x = 0.2$ in (b) and for $x = 0.3$ in (c). The following characteristics can be seen: (i) The Stokes shift decreases as a whole with the external magnetic field, since the magnetic polaron becomes unstable with increasing the magnetic field, as discussed by many authors [24]. (ii) Even without the external

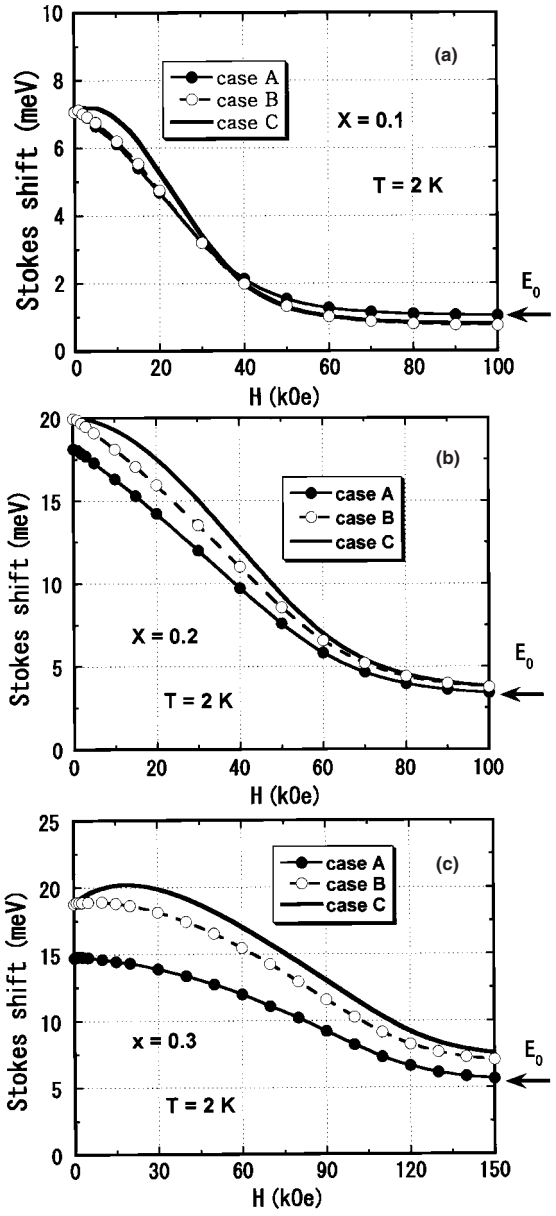

Figure 5. The Stokes shift calculated at 2 K is shown as a function of H for $x = 0.1$ in (a), $x = 0.2$ in (b) and $x = 0.3$ in (c). The horizontal arrow shows the localization energy E_0 expected from the nonmagnetic part of the APFs. Consult the text for the definition of cases A, B and C.

magnetic field the Stokes shift in cases B and C differs from that in case A as seen in figure 5 and later in figure 7. For $Cd_{1-x}Mn_xTe$, as already mentioned, the EXMPs affected by the APFs are localized in the region where the local composition of Mn ions is less than the averaged one; the EXMPs experience the effective Mn concentration $x_{\rm eff}(\vec{r})$ differing from the average one $x_{\rm eff}$. The above difference at 0 kOe is thus due to the effect of the magnetic part of the APFs induced by *the inhomogeneous internal magnetic field* produced by the EXMPs. (iii)

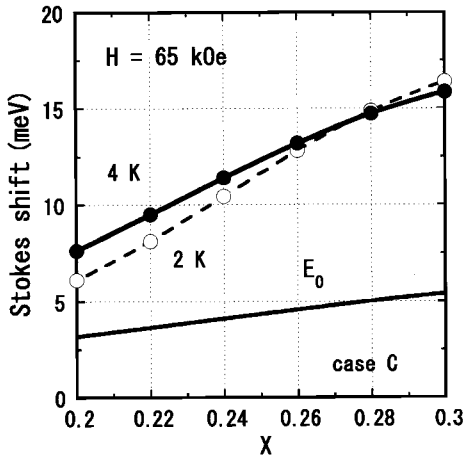

Figure 6. The Stokes shift calculated at 65 kOe for 2 and 4 K is shown from $x = 0.2$ to 0.3 for case C. The solid line shows the Stokes shift E_0 expected as a result of the nonmagnetic part of the APFs.

The overall difference in the Stokes shift between cases A and B (C) is rather small for $x = 0.1$ compared with that for $x = 0.2$ and 0.3, since the effect of the magnetic part of the APFs is relatively small for $x = 0.1$ as discussed in section 3. (iv) A broad peak at about 30 kOe for $x = 0.3$ in case C (figure 5(c)) is the crossover effect due to the increase in the APFs (figure 4(a)) and the destabilization of the EXMPs with increase in the magnetic field. The behaviour may be related to the experimental result for $Cd_{0.82}Mn_{0.18}Te$ under the magnetic field reported in [25].

Let us now turn to the region of high magnetic field where the magnetic polaron vanishes. (v) We see in figure 5 that the Stokes shift in the cases B and C calculated at the high magnetic field limit (HMFL) differs from that calculated in case A. Since the magnetic part of the APFs is not included in case A, the Stokes shift calculated at HMFL in case A approaches the localization energy due to the nonmagnetic part of the APFs shown by the horizontal arrow in figure 5. On the other hand, the Stokes shift for cases B and C includes the effects of the magnetic part of the APFs. (vi) In closer observations at HMFL, the difference in the Stokes shift between cases A and B (C) is less than about 0.4 meV for $x = 0.1$ and 0.2; however, the difference increases to about 2 meV for $x = 0.3$. This is due to the magnitude of $\frac{\mathrm{d}}{\mathrm{d}x}x_{\mathrm{eff}}$ as discussed in section 3. The Stokes shift calculated at HMFL is now compared with the localization energy obtained by the experiment shown in section 2. Here, we remember that the localization energy shown by the closed circles in figure 1 is derived from the nonmagnetic part of the APFs, while that by the open circles is derived from both the non-magnetic and the magnetic parts of the APFs. As already mentioned at (vi) above, the difference in the Stokes shifts with and without the magnetic part of the APFs, calculated at HMFL, is small for $x = 0.1$ and 0.2. Then, the calculation for $x = 0.1$ is consistent with the experimental result mentioned in item (ii) in section 2. For $x = 0.2$, however, the calculation, seems to be far from the experimental result of item (iii) in section 2. Concerning this disagreement, we would like to suggest that the magnetic field of 65 kOe applied at 4.2 K [10] does not produce saturated magnetizations for $x = 0.21$ (see figure 5(b)). This implies that the Stokes shift obtained in the experiment includes the localization energy due to the formation of the EXMPs. For verification, we calculated the Stokes shift at 65 kOe at 2 and 4 K, showing in figure 6 as a

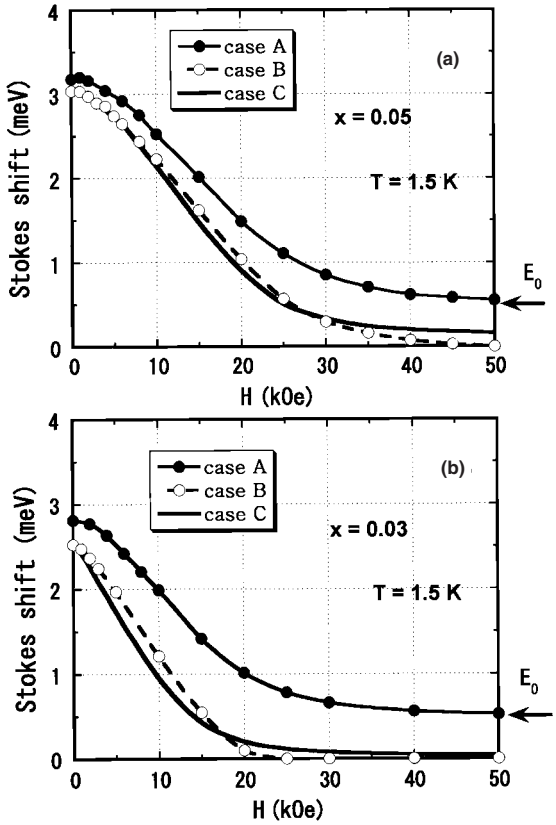

Figure 7. The Stokes shift calculated at 1.5 K is shown as a function of H for $x = 0.05$ in (a) and $x = 0.03$ in (b). The horizontal arrow shows the localization energy E_0 expected as a result of the nonmagnetic part of the APFs, which is set to be 0.5 meV in the calculation. Consult the text for the definition of cases A, B and C.

function of $x = 0.1$–0.3 for case C; the Stokes shift at 4 K for $x = 0.21$ becomes about 8 meV at 65 kOe. The calculated result, then, is consistent with the experiment, which may verify the above suggestion from the experiment for $x = 0.21$.

Now we extend the calculation to the case of a low Mn concentration, less than $x = 0.1$. The Stokes shift calculated at 1.5 K is shown for $x = 0.05$ in figure 7(a) and 0.03 in (b). In the calculation, we set the localization energy $E_0(\xi_0)$ caused by the nonmagnetic part of the APFs to be 0.5 meV so as to reproduce the Stokes shift observed at 0 kOe. This is an intermediate value between the two energies for the band edge smearing, which are shown by the solid line and the closed squares in figure 1. In the region of low Mn concentration, the effect of the magnetic part of the APFs causes the APFs as a whole to reduce considerably with increasing magnetic field as discussed in section 3 (see figure 4). This is clearly seen in figure 7: with increase of H, the Stokes shift calculated for cases B and C with the magnetic part of the APFs decreases rapidly compared with that for case A without the magnetic part of the APFs. For $x = 0.05$, the calculated Stokes shift becomes less than 0.2 meV at $H > 40$ kOe, which is consistent with the recent photoluminescence experiment by Kamohara *et al* for $Cd_{0.945}Mn_{0.055}Te$ [26]. Furthermore, for $x = 0.03$, the Stokes shifts in cases B and C become quite small at $H > 20$ kOe: the excitons become rather extended in the high magnetic field

even when the EXMPs are localized at 0 kOe with the assistance of the APFs. By a time-resolved photoluminescence experiment at 4.2 K in $Cd_{0.97}Mn_{0.03}Te$ [11], the shift of the peak energy (or the Stokes shift) is 2–3 meV at 0 kOe, while the shift becomes less than 0.1 meV at 70 kOe. The calculation is thus consistent with this experiment associated with item (iv) in section 2. In this way, we conclude that the APFs become quite small as a whole due to the magnetic part of the APFs when a relatively high magnetic field is applied to $Cd_{1-x}Mn_xTe$ with a low Mn concentration.

5. Summary

We have investigated the effect of an external magnetic field on the APFs in DMSs within the molecular field approximation, taking the example of $Cd_{1-x}Mn_xTe$. Because of the magnetic part of the APFs caused by the compositional fluctuations of Mn ions and the sp–d exchange interaction, the APFs in DMSs depend on the magnetic field and the temperature as well as on the concentration of the magnetic ions, producing the peculiar behaviours discussed in this paper. Calculation of the EXMPs weakly bound to the APFs was also performed, and was compared with the L_2 photoluminescence experiment with the purpose of revealing the effects of the magnetic part of the APFs in the experimental results. The characteristics of $Cd_{1-x}Mn_xTe$ discussed here may be expected in many other DMSs, since ξ_0 is positive in many DMSs as in $Cd_{1-x}Mn_xTe$. On the other hand, in $Zn_{1-x}Mn_xS$ with a negative ξ_0, different characteristics from $Cd_{1-x}Mn_xTe$, as expected from the discussion in section 3, may be realized.

Acknowledgments

This work started at the Advance Material Laboratory, National Institute for Material Science, Tsukuba, Japan, and continued at the Joint Research Program supported by the Institute for Solid State Physics (ISSP), University of Tokyo, Kasiwanoha, Chiba, Japan. The author would like to express his sincere thanks to Professor S Takeyama at Tokyo University for stimulating discussions. He also wishes to thank the members of the ultra-high magnetic field laboratory, ISSP, for their hospitality.

References

[1] See, for example, Furdyna J K 1988 *J. Appl. Phys.* **64** R29
[2] Halperin B I and Lax M 1966 *Phys. Rev.* **148** 722
Lifshitz I M 1967 *Zh. Eksp. Teor. Fiz.* **53** 743
Lifshitz I M 1968 *Sov. Phys.—JETP* **26** 462 (Engl. Transl.)
[3] Baranovskii S D and Efros A L 1978 *Fiz. Tekh. Poluprov.* **12** 2233
Baranovskii S D and Efros A L 1978 *Sov. Phys.—Semicond.* **12** 1328
[4] Umehara M 2003 *Phys. Rev.* B **68** 193202
[5] Takeyama S, Adachi S, Takagi Y and Aguekian V F 1995 *Phys. Rev.* B **51** 4858
See also [8] and [9]
[6] Itoh T and Komatsu E 1988 *J. Lumin.* **38** 266
[7] Mackh G, Ossau W, Yakovlev D R, Waag A, Landwehr G, Hellmann R and Gobel E O 1994 *Phys. Rev.* B **49** 10248
[8] See, for $x = 0.12$, Takeyama S, Adachi S, Takagi Y, Karczewski G, Wojtowicz T, Kossut J and Karasawa T 1999 *Mater. Sci. Eng.* B **63** 111
[9] See, for $x = 0.15$, Takeyama S, Karasawa T and Aguekian V F 1997 *The 2nd Symp. on the Physics and Application of Spin-Related Phenomena in Semiconductors* p 10 (Exdended Abstracts)
For $x = 0.18$, Takeyama S, Takagi Y, Karasawa T and Aguekian V F 1998 *J. Cryst. Growth* **184/185** 917

[10] See, for $x = 0.1$, Nogaku M, Takahashi M, Shen J X and Oka Y 1999 *The 5th Symp. on the Physics and Application of Spin-Related Phenomena in Semiconductors* p 27 (Extended Abstracts)
See, for $x = 0.21$, Shen J X, Debnath M C, Souma I, Shirado E, Sato T and Oka Y 1998 *The 4th Symp. on the Physics and Application of Spin-Related Phenomena in Semiconductors* p 149 (Extended Abstracts)
[11] Nogaku M, Pittini R, Sato T, Shen J and Oka Y 2001 *J. Appl. Phys.* **89** 7287
Nogaku M, Shen J X, Pittini R, Sato T and Oka Y 2001 *Phys. Rev.* B **63** 153314
[12] Minami F and Era K 1987 *J. Lumin.* **38** 84
[13] Komatsu E 1986 *Master Thesis* Department of Science, Tohoku University, Sendai, Japan
[14] Cohen E and Sturge M D 1982 *Phys. Rev.* B **25** 3828
[15] For example, Chen C-J, Qu M, Hu W, Zhang X, Lin F, Hu H-B, Ma K-J and Giriat W 1991 *J. Appl. Phys.* **69** 6114
[16] Gaj J A, Planel R and Fishman G 1979 *Solid State Commun.* **29** 435
See also [15]
[17] Shapira Y, Foner S, Ridgley D H, Dwight K and Wold A 1984 *Phys. Rev.* B **30** 4021
[18] Fatah J M, Piorek T, Harrison P, Stirner T and Hagston W E 1994 *Phys. Rev.* B **49** 10341
[19] See Appendix A in Umehara M 2003 *Phys. Rev.* B **67** 035201
[20] Umehara M 2002 *Phase Transit.* **75** 1027
[21] Goede O and Heimbrodt W 1988 *Phys. Status Solidi* b **146** 11
[22] Hagston W E, Stirner T and Miao J 1997 *J. Appl. Phys.* **82** 5653
[23] Aguekian V F, Gridneva L K and Serov A Yu 1993 *Solid State Commun.* **85** 859
[24] See, for example, Akinaga H, Takita K, Sasaki S, Takeyama S, Miura N, Nakayama T, Minami F and Inoue K 1992 *Phys. Rev.* B **46** 13136
See also [7]
[25] Takeyama S, Adachi S, Takagi Y and Aguekian V F 1995 *Phys. Rev.* B **52** 1444
[26] Kamohara T 2003 *Master Thesis* Department of Science, Chiba University, Chiba, Japan